

## Compatibility of VLBI Measurements from Different Networks Using an Analysis of Variance Model and Their Impact on Baseline Rates

H. Bâki Iz\*

Department of Land Surveying and Geo-Informatics  
The Hong Kong Polytechnic University, Hong Kong, China

and

B. A. Archinal

USGS, Astrogeology Team Planetary Geomatics Group, Flagstaff, AZ, U.S.A.

(Received June 14, 2001; Revised December 10, 2001; Accepted December 20, 2001)

### 分散分析モデルを用いた異なる VLBI 観測網間の 計測の整合性およびその基線変化率への影響の検討

H. バキイズ<sup>1)</sup>・B. A. アーキナル<sup>2)</sup>

1) 香港科学技術大学, 2) 米国地質調査所

(2001 年 6 月 14 日受付, 2001 年 12 月 10 日改訂, 2001 年 12 月 20 日受理)

#### 要 旨

さまざまな VLBI 計測において副産物として得られる基線観測結果はプレート運動の結果としての基線長変化の監視に定常的に用いられている。ここでは、実験条件の変化や異なる観測網の幾何的配置により、異なる VLBI 観測網の基線解に有意な差異があるかどうかを調査した。また、基線解の時間変化に影響を及ぼす可能性についても評価した。分散モデル解析 (ANOVA) はこの目的のために準備した。調査した 17 の基線の内、5 本の基線観測で 0.001 p-level の不整合が見出された。しかし、この 5 本の基線の内、異なる観測網の不均一性によりもたらされたと考えられる基線は 1 本だけであった。(訳: 編集委員)

#### Abstract

Baseline observations, byproducts of various VLBI measurement sessions (experiments) from different VLBI networks, are routinely used to monitor changes in the baseline lengths as a result of plate motions. In this study, we investigate whether the baselines from different VLBI networks are significantly different from each other, which may be due to the changing experimental conditions of sessions or differing network geometries. We also assess their potential impact on the baseline rates. An analysis of variance model (ANOVA) is constructed for this purpose. Out of seventeen baselines examined five baselines measurements are found to be incompatible with each other at 0.001 *p-level*. However out of five baseline rates, only one baseline rate was significantly affected by the inhomogeneities induced by different networks.

\* Fax: (852)2330 2994, E-mail Internet: lshbiz@polyu.edu.hk

## 1. Introduction

Tectonic rates are now solved for on a global basis using Very Long Baseline Interferometry (VLBI) data, obtained by NASA's Goddard Space Flight Center, and other national and international participants. Baseline components recovered from these global solutions are now routinely used to determine baseline lengths and monitor changes due to the plate motions (Ma and Ryan, 1998).

The global solutions, through complex models, provide information, among others, about site (station) positions and velocities from a simultaneous solution using all available VLBI data. A special global solution is made to produce baseline evolution from the ensemble of VLBI data with no a priori information about plate motions. In this process the station coordinates are adjusted for each observation session together with a common set of source coordinates and an a priori EOP series. Subsequently a set of site coordinates referring to a common epoch and their velocities are estimated from the session station coordinates. The estimated site positions and velocities all refer to a common VLBI reference frame realized at a given epoch (ibid).

Because the site coordinates and velocities are dependent on how the reference frame is realized, further analyses of results using the baseline observations from session solutions are informative because, by their very nature, they are free from various unknown systematic effects that may be present in the site positions (baseline lengths are invariant with respect to the rotation and translation of the underlying coordinate system). Direct estimation of the baseline rates from the baseline measurements is simple and provides a cross check for the quality of global solutions. They offer exploratory information that may otherwise be buried in the complexity of the global solutions.

## 2. VLBI session/network

Geodetic applications of VLBI involve measurement of baseline projections in the direction of the radio sources from at least two stations. A series of antennas from different stations scan the sky to observe radio sources above a lower elevation limit producing as many observations as possible in as many directions at each site as possible for a subsequent least-squares analysis. A typical experiment uses 20 to 30 sources and usually lasts 24 hours. A group of observations from a station antenna belongs to a *session* or equivalently to an *experiment*. All the station antennas at different locations participating to a session (experiment) form a *network*. Observation of a multitude of sources during a 24-hour session enables separation of parameters such as nutation and polar motion and UT1. The results are then reviewed after the experiment to check the consistency of data from each source. Whereas the baseline and the position of the sources can be considered constant for a one-day experiment, other parameters are not. The atmosphere and clocks that affect the measurements vary in time. Currently, the propagation delays are the significant error source in geodetic VLBI that limits its accuracy. Although observing sources at two different frequencies eliminates most of the effect of the

ionosphere, delays due to the earth's troposphere are much harder to deal with. The maser clocks, which control VLBI data sampling, and other instrumentation, are also not perfect. They have both random and systematic drifts. Most of the systematic drifts are easily modeled and solved for in the analysis (Shaffer, 1995).

Every effort is taken for generating a consistent set of observations through periodic calibrations to free them from systematic effects, to achieve a consistent set of measurements within each session. In practice though, the observing geometry varies, in e.g. some sources being observed only in one part of the sky, introducing systematic errors due to tropospheric and ionospheric effects. There are also indications that global VLBI networks systematically give different results from regional ones, since global networks are more tightly constrained in the vertical, and so there may be some systematic differences in comparison to smaller networks. It is also possible that there may be unknown systematic variations small enough to be buried in the noise level of the measurements that span a short period of time but are influential over longer periods. Occasionally there are obvious "discontinuities" at a given antenna, when the antenna is overhauled, the azimuth track is replaced, the antenna is replaced by a nearby antenna, or even an earthquake. These factors may adversely effect the accurate estimation of baseline rates using baseline measurements generated by different networks.

In this study we investigate whether baseline measurements from a network are significantly different from the other networks and the potential impact of this on estimated baseline rates.

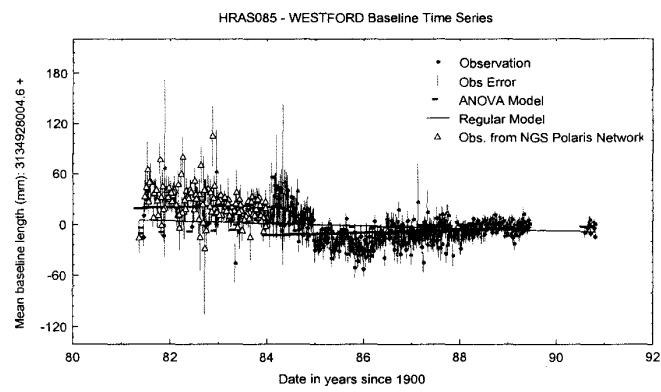
### 3. Baseline measurements and rates

Although we have examined 17 baselines selected for having large number of observations from different sessions to detect the compatibility of measurements from various networks and assessed their influence on baseline rates, we will focus only on three baselines here for brevity (Figure 1). These are:

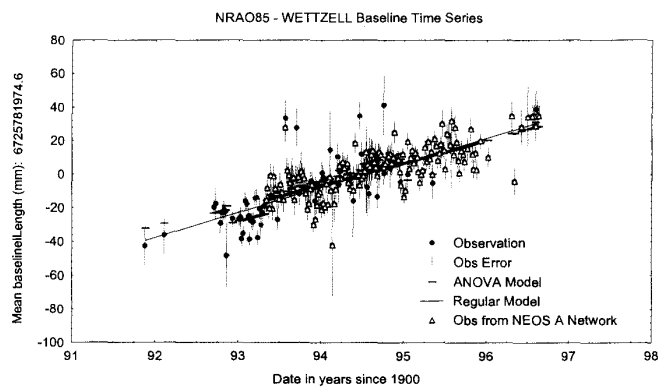
HRAS–Westford baseline is denoted by HW. HRAS 085 is now a removed 85-foot antenna at the former Harvard Radio Astronomy Station, near Ft. Davis, TX. It was later replaced by the NRAO VLBA antenna there, FD–VLBA. The Westford antenna is located at Westford, Massachusetts, continuing earlier observations from Haystack Observatory, HAYSTACK. The HW baseline consists of 603 measurements (Table 1 and Figure 1) generated by 10 different network solutions distributed over ten years during 1981 to 1991. NGS Polaris and IRIS A networks dominate most of the measurements (Figure 2a). Earlier data, until 1985, are noisier than the rest of the measurements partly because Richmond antenna in the network did not come on-line until 1984; hence before that time there were less data available.

NRAO85–Wetzell baseline, NW, is generated by the measurements from an 85-foot antenna no. 3, operated by NRAO in Green Bank, West Virginia (this antenna was later replaced by a 20-meter antenna, NRAO20) and the one in Wetzell, Germany. The 222 NW baseline measurements span approximately 5 years and consist of 9 different networks (Table 1 and

1a



1b



1c

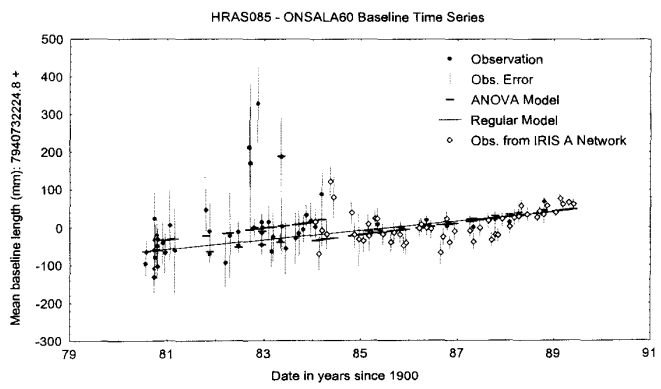


Fig. 1 Time series of VLBI baseline measurements and their errors from different sessions.

Table 1. Model solutions for seventeen baselines. Standard deviations are at one sigma level. Only the first three baseline solutions are discussed in detail in the manuscript. R stands for rejected, NR is for non-rejected null-hypothesis test.

| Baseline              | Estimated Slope (mm/yr) |                       |                |                 |                       |      | Average<br>b.l.<br>noise** | $F^{***}$ | Null<br>Hyp.<br>$\alpha = 0.001$ |
|-----------------------|-------------------------|-----------------------|----------------|-----------------|-----------------------|------|----------------------------|-----------|----------------------------------|
|                       | Regular<br>Model        | $\hat{\sigma}^*$ (DF) | NUVEL<br>Model | ANOVA<br>Model  | $\hat{\sigma}^*$ (DF) |      |                            |           |                                  |
| HRAS085-<br>WESTFORD  | $-1.5 \pm 0.3$          | 1.76(601)             | 0.0            | $+1.6 \pm 0.3$  | 1.45(591)             | 10.6 | 0.126<br>3.205             | R         |                                  |
| NRAO85-<br>WETTZELL   | $14.8 \pm 0.7$          | 1.63(220)             | 18.2           | $13.4 \pm 1.0$  | 1.59(212)             | 7.2  | 0.088<br>3.669             | NR        |                                  |
| HRAS085-<br>ONSALA60  | $12.3 \pm 1.1$          | 1.29(110)             | 15.3           | $15.5 \pm 1.6$  | 1.24(103)             | 36.2 | 0.068<br>4.123             | NR        |                                  |
| ALGOPARK-<br>FORTLEZA | $-1.2 \pm 1.5$          | 1.33( 26)             | 1.5            | $-0.3 \pm 1.9$  | 1.40( 20)             | 8.2  | 0.015<br>8.230             | NR        |                                  |
| ALGOPARK-<br>KOKEE    | $7.9 \pm 0.9$           | 1.54( 72)             | 3.6            | $7.5 \pm 1.4$   | 1.55( 66)             | 9.8  | 0.016<br>5.754             | NR        |                                  |
| ALGOPARK-<br>MATERA   | $15.8 \pm 0.5$          | 1.14( 38)             | 18.6           | $15.9 \pm 2.4$  | 1.18( 33)             | 9.7  | 0.005<br>7.748             | NR        |                                  |
| ALGOPARK-<br>WETTZELL | $18.3 \pm 0.4$          | 1.63(111)             | 18.6           | $17.7 \pm 1.1$  | 1.54(103)             | 7.2  | 0.049<br>4.436             | NR        |                                  |
| FORLEZA-<br>SANTIA12  | $-15.7 \pm 1.2$         | 1.00( 51)             | 0.0            | $-16.6 \pm 1.6$ | 1.00( 46)             | 11.9 | 0.005<br>7.151             | NR        |                                  |
| GILCREEK-<br>HATCREEK | $-9.6 \pm 0.6$          | 1.26( 97)             | 0.0            | $-9.6 \pm 0.8$  | 1.23( 90)             | 10.8 | 0.031<br>4.927             | NR        |                                  |
| GILCREEK-<br>KASHIMA  | $1.7 \pm 0.2$           | 1.56(173)             | 0.0            | $0.48 \pm 0.4$  | 1.48(162)             | 10.2 | 0.106<br>3.537             | NR        |                                  |
| GILCREEK-<br>KAUAI    | $-45.8 \pm 0.2$         | 1.43(406)             | -45.4          | $-45.9 \pm 0.3$ | 1.36(388)             | 8.0  | 0.218<br>2.674             | R         |                                  |
| GILCREEK-<br>MOJAVE12 | $-10.8 \pm 0.2$         | 1.62(300)             | 0.0            | $-10.6 \pm 0.3$ | 1.49(282)             | 5.1  | 0.217<br>2.710             | R         |                                  |
| HRAS-<br>WETTZELL     | $14.0 \pm 0.7$          | 1.17(414)             | 15.7           | $14.2 \pm 0.7$  | 1.17(410)             | 26.4 | 0.005<br>6.032             | NR        |                                  |
| KAUAI-<br>RICHMOND    | $28.0 \pm 1.8$          | 1.35(129)             | 27.3           | $28.3 \pm 1.9$  | 1.36(125)             | 16.4 | 0.001<br>8.086             | NR        |                                  |
| ONSALA-<br>WESTFORD   | $17.1 \pm 0.2$          | 1.89(229)             | 17.6           | $16.8 \pm 0.4$  | 1.64(208)             | 10.6 | 0.251<br>2.594             | R         |                                  |
| RICHMOND-<br>WETTZELL | $14.2 \pm 0.4$          | 1.51(538)             | 17.1           | $14.2 \pm 0.4$  | 1.52(530)             | 17.7 | 0.050<br>4.094             | NR        |                                  |
| WESTFORD-<br>WETTZELL | $17.0 \pm 0.1$          | 1.85(867)             | 18.9           | $17.4 \pm 0.2$  | 1.80(831)             | 9.5  | 0.383<br>2.037             | R         |                                  |

\*A posteriori variance of unit weight.

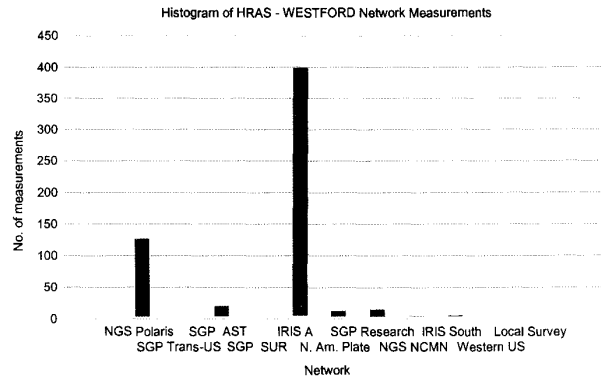
\*\*Mean of the standard deviations of individual baseline lengths (baseline errors) from session solutions in mm.

\*\*\* $F$  values for upper and lower tail. Null hypothesis test is performed using upper and lower tails and  $p$  values.

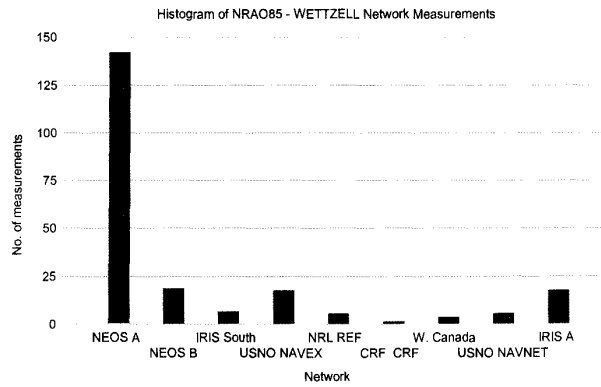
Figure 1). NEOS A network dominates 70 percent of the measurements on this baseline (Figure 2b). Some 16 measurements from IRIS A network however are taken place during 1993, a period early enough to be influential in the solution despite their numbers (Figure 2b).

Finally HRAS085–Onsala, HO baseline is formed by the participating station in Onsala, Sweden. The HO baseline measurements are sparsely distributed over 5 years as compared

2a



2b



2c

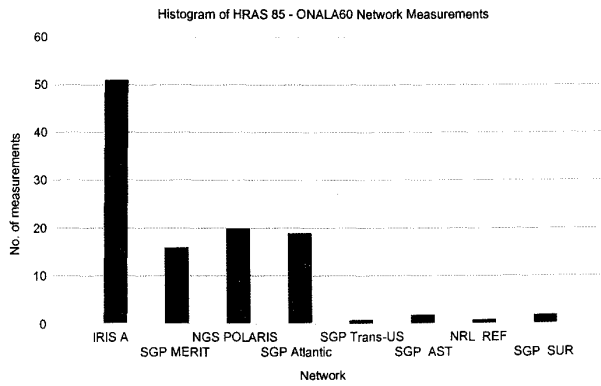


Fig. 2 Bar charts of Network Measurements.

with the previous two groups of baseline measurements. Nevertheless, among 8 networks, IRIS-A network accounts for almost 50 percent of the 112 measurements (Table 1 and Figure 2c). The first three years of measurements are noisier than the remaining observations with some outlying observations with large errors (Figure 1c).

The last two baselines typify the analysis results of the remaining baselines whereas the first case is unique among the others.

#### 4. Estimation of baseline rates

The typical approach for estimating baseline rates can be described as follows.

$$\begin{aligned} y_1 &= a + bt_1 + u_1 \\ y_2 &= a + bt_2 + u_2 \\ &\vdots \\ y_n &= a + bt_n + u_n, \end{aligned} \quad (1)$$

which can be expressed in a matrix notation as

$$\mathbf{y} = \mathbf{A}\mathbf{x} + \mathbf{u}. \quad (2)$$

In the above expression  $\mathbf{y}$  is the  $n$ -vector of baseline observations, where  $n$  is the total number of observations. The unknown parameter vector  $\mathbf{x}$  is composed of the intercept and the slope (baseline rate per year) parameters ( $a$  and  $b$ ). The  $n$ -vector of disturbances (errors),  $\mathbf{u}$ , has the following assumed statistical properties,

$$E(\mathbf{u}) = \mathbf{0}, \quad E(\mathbf{u}\mathbf{u}^T) = \text{diagonal}(\sigma_i^2) = \sigma_u^2 \mathbf{W} \quad i = 1, \dots, n, \quad (3)$$

where  $\sigma^2$  is the *a priori* variance of unit weight which is assumed to be one. This value will be subsequently replaced by the estimated *a posteriori* variance of unit weight.  $\mathbf{W}$  is the  $n \times n$  diagonal weight matrix of observations<sup>1</sup>.  $\mathbf{A}$  is the  $n \times 2$  design matrix. The first column of the design matrix is all equal ones. The second column is composed of the corresponding epoch of observation,  $t_i$ , expressed in Julian years that are shifted by an appropriate number of years in order to work with less number of digits for a well-conditioned solution.

A generalized (weighted) least squares solution to the equation (2) is well-known and is given by,

$$\hat{\mathbf{x}} = (\mathbf{A}^T \mathbf{W}^{-1} \mathbf{A})^{-1} \mathbf{A}^T \mathbf{W}^{-1} \mathbf{y}, \quad (4)$$

where  $\hat{\mathbf{x}}$  is the 2-vector of the least-square estimate of the unknown parameter vector  $\mathbf{x}$  which consists of the intercept and the slope. The estimated variance-covariance matrix of the adjusted parameters is given by

<sup>1</sup> Strictly speaking the weight matrix is not diagonal. Nevertheless, the impact of serial correlations (autocorrelations) on the baseline rates was estimated and found to be negligible in Iz, and Y. Chen (1999).

$$\Sigma_{\hat{a}} = \hat{\sigma}^2 (\mathbf{A}^T \mathbf{W}^{-1} \mathbf{A})^{-1}, \quad (5)$$

where  $\hat{\sigma}^2$  is the *a posteriori* variance of unit weight. Within the framework of the analysis of variance, ANOVA, this quantity is also known as *the total variance*, and is given by

$$\hat{\sigma}^2 = (\mathbf{y} - \mathbf{A}\hat{\mathbf{x}})^T \mathbf{W} (\mathbf{y} - \mathbf{A}\hat{\mathbf{x}}) / (n - 2), \quad (6)$$

where the circumflex on the variables indicates that they are estimated quantities.

Figure 1 shows the baseline measurements and their errors as reported by the NASA's GSFC VLBI Solution 1102g–August 1998. We estimated the baseline rates using the above model, which are given in Table 1. They are the same as reported in the same solution document. Overall, the estimated rates agree well with the geological rates as estimated through the NUVEL-1 model (DeMets *et al.*, 1994).

One of the intrinsic assumptions in the above solution is that all the observations from different networks have similar statistical properties, i.e. they are compatible with each other. Assume for a moment that there are no plate motions affecting the baselines or the baselines are corrected for the plate motions. In this case we do not expect the means of the observations from different networks to be statistically different from each other.

To test the validity of this assumption we can compute the variance of measurements from different networks and pool them to obtain the internal variance (variance within means). We can also compute the variance among the means using the mean of all measurements from all networks and the means of measurements from each network. This gives us the external variance. We expect that the internal and external variances will not differ from each other if the measurements from different networks have a common variance. We can test whether the internal variance and external variance are statistically different from each other using their ratios which is *F* distributed if the observations are assumed to be normally distributed. This scenario is the basis of the well-known analysis of variance (ANOVA). However, in this study we need a modified formulation of this scenario to take into account the time dependent variations in the baseline lengths that are common to all baseline measurements, and their correlation with the baseline means (intercepts). This is the topic of the next section. The following derivations are motivated by the ANOVA methods discussed in Bjerhammer (1973) for rank deficient linear models.

## 5. Analysis of variance model

The intercept parameter discussed above can also be computed in two steps. In the first step, a set of preliminary intercept parameters is obtained using the baseline measurements from each network. These parameters differ from network to network but share the same slope parameters on the same baseline (obviously, the station motions due to the motion of tectonic plates do not depend which network observes the baseline). A common intercept parameter is obtained from the estimated intercepts of preliminary network solutions in the second step.



with

$$\mathbf{C}' := \begin{bmatrix} 1 & 1 & 1 & \cdots & 0 \\ 0 & 0 & 0 & \cdots & 1 \end{bmatrix}, \quad (13)$$

where  $\mathbf{C}$  is the  $n \times (p+1)$  coefficient matrix,  $\mathbf{X}$  is the  $(p+1)$ -vector of  $p$  intercepts and a slope and  $\mathbf{x}$  is the 2-vector of intercept and slope parameter. Substituting (12) into (8) we obtain a set new of observation equations from which the final intercept and slope can be estimated

$$\mathbf{y} = \mathbf{BCx} + \mathbf{u}. \quad (14)$$

The least square estimate  $\hat{\mathbf{x}}$  is  $\mathbf{x}$  obtained from

$$\hat{\mathbf{x}} = (\mathbf{C}^T \mathbf{B}^T \mathbf{W}^{-1} \mathbf{BC})^{-1} \mathbf{C}^T \mathbf{B}^T \mathbf{W}^{-1} \mathbf{y}. \quad (15)$$

The error estimate for the disturbances based on the parameter estimates of this solution is

$$\hat{\mathbf{u}} = \mathbf{y} - \mathbf{C}_0 \mathbf{W}^{-1} \mathbf{y} \quad \text{with} \quad \mathbf{C}_0 := \mathbf{BC}(\mathbf{C}^T \mathbf{B}^T \mathbf{W}^{-1} \mathbf{BC})^{-1} \mathbf{C}^T \mathbf{B}^T. \quad (16)$$

Now, using the partial error estimate of the final solution given by

$$\Delta \mathbf{u} = \hat{\mathbf{u}} - \tilde{\mathbf{u}} = \mathbf{B}_0 \mathbf{W}^{-1} \mathbf{y} - \mathbf{C}_0 \mathbf{W}^{-1} \mathbf{y} \quad (17)$$

the external variance of the solution is obtained (following the definition of the external variance) as,

$$\hat{\sigma}_{\text{ext}}^2 := (\mathbf{y}' \mathbf{W}^{-1} \mathbf{B}_0 \mathbf{W}^{-1} \mathbf{y} - \mathbf{y}' \mathbf{W}^{-1} \mathbf{C}_0 \mathbf{W}^{-1} \mathbf{y}) / [(p+1) - 2]. \quad (18)$$

## 6. Statistical testing

The *internal* and *external* variances are independent from each other because the expected value of the partial error estimates times the error estimates given by (16) and (17) is zero. Hence, for normally distributed observations, the variance ratios will be  $F$ -distributed.

The calculated value of the variance ratio in the following expression is  $F$ -distributed with  $(p+1) - 2$  degrees of freedom in the numerator and  $n - (p+1)$  degrees of freedom in the denominator

$$F = \hat{\sigma}_{\text{ext}}^2 / \hat{\sigma}_{\text{int}}^2. \quad (19)$$

We will use the above variance ratio to test the equality of the variances using a two-tailed hypothesis testing procedure at a given  $p$ -level (statistical significance) which represents the probability of error that is involved in accepting our observed result as valid, that is, as "representative of the population" (or one tailed tests to determine which one is larger than the other). When the computed variance ratio exceeds its corresponding theoretical value the null-hypothesis is rejected at the given  $p$ -level.

Let us now look at its application to the set of previously discussed VLBI baselines.

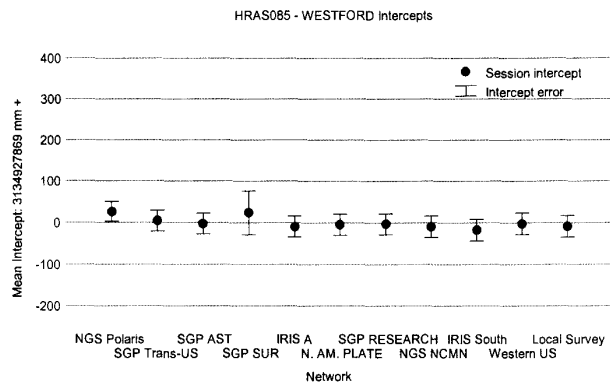
## 7. Numerical Results and Conclusion

We applied the above testing procedure to the selected baselines. The  $F$ -test results for the HW baseline indicate that the observations that belong to different networks are not compatible. They are statistically different from each other at 0.001  $p$ -level. Given the distribution of the data depicted in Figure 1a and Figure 2a this result is not surprising. The estimated intercepts from the ANOVA model show that the result is due to the incompatibility of the measurements from two different networks that dominate the solution. Incompatibilities are also present in other network observations. Although in Figure 3a the variation of the intercepts are not markedly different, the small magnitude of the corresponding error estimates (the average measurement noise is 10.6 mm) seems to be enhancing the existing variability among them (signal-to-noise ratio). However, the major reason for the small intercept errors displayed in Figure 3a, is because the ANOVA model fits better to the baseline measurements than the fit of the regular model where the measurements from different networks are assumed to be compatible hence represented by a single intercept parameter. This model's rate is in opposite direction of the regular model's rate. These results however, because there is little overlap between two major network data (NGS and IRIS A), do not rule out a short-term slippage in the baseline length instead of a network dependent incompatibility.

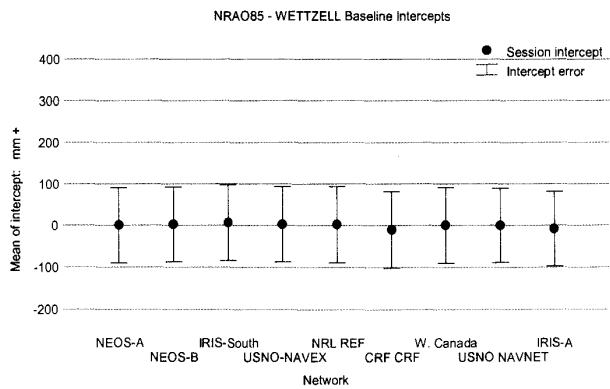
The NW baseline measurements from different networks are in agreement at 0.001  $p$ -level. Note that the intercept errors, on the average, are three times as large when compared with the HW baseline intercepts despite the small measurement errors (the average measurement noise is 7.2 mm). However, the intercepts that belong to different networks and their errors displayed in Figure 3b are in close agreement with each other and homogeneously distributed among different networks. In this solution, a potential problem due to the incompatibility of the IRIS A network with the remaining ones is offset by the presence of few observations from USNO NAVEX network at the beginning of the period (it can be shown that linear regression model solutions are dominated by the measurements at the beginning and at the end of experiments much more than the ones in the middle-in this particular case, a solution without USNO NAVEX measurements gives a significantly different baseline rate). The estimated baseline rates from both regular and ANOVA models are in close agreement in magnitude and direction.

HW and HO baselines share the HRAS085 station and have overlapping periods of observations. Despite these commonalities between the series, the  $F$ -test results for the HO baseline solution indicate the session observations are compatible at the 0.001  $p$ -level but not for the HW baseline session observations. One apparent reason for this result is due to the large noise of baseline observations from all the networks for the HO baseline. The average measurement error is 36.2 mm, which is five times larger than the NW measurement errors. Consequently, the apparent discordance among the estimated intercepts from different networks (Figure 3c) is buried in the noise of baseline observations from all networks. The other reason is because

3a



3b



3c

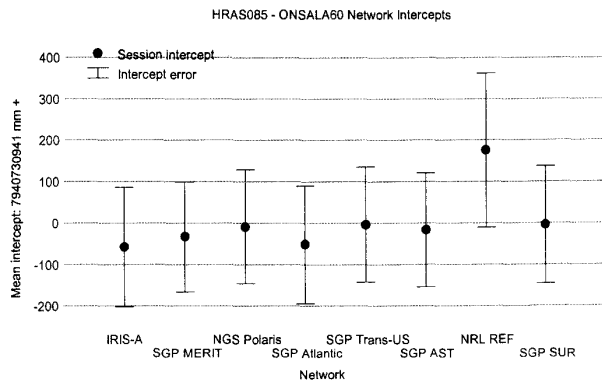


Fig. 3 Estimated intercepts from different networks and their errors.

of the varying number of observations in different sessions. NRL REF session intercept, for instance, is markedly different than the other estimates. This session, however, contributes only one observation to the total solution. The estimated baseline rate from the ANOVA model for the HO baseline is in better agreement with the NUVEL-1 rates (Table 1).

We applied the above test procedure to the measurements from 14 additional baselines. Out of 14 baselines, the test results indicate that 10 baselines' measurements from different networks are compatible with each other. The remaining 4 baselines contain statistically incompatible measurements from different networks/sessions. Nevertheless, their impacts on the baseline rates are negligible. This exercise will need to be repeated in the future because of the possible improvements in the noise levels of newer measurements from different networks.

### Acknowledgements

This research has made use of NASA Goddard Space Flight Center's VLBI terrestrial reference frame solution number 1102g, 1998 August. This study was supported by the Hong Kong Polytechnic University internal research grant A-PC78. Careful comments by two referees markedly improved the accuracy of the manuscript and are gratefully acknowledged.

### References

- Bjerhammer, A. (1973): *Theory of Errors and Generalized Matrix Inverses*, Elsevier Scientific Publishing Company, New York.
- DeMets, C., R. G. Gordon, D. F. Argus and S. Stein (1994): Effect of recent revisions to the geomagnetic time scale on estimates of current plate motions, *Geophys. Res. Lett.*, **21**, 2191-2194.
- Iz, H. B. and Y. Chen (1999): VLBI rates with first order autoregressive disturbances, *Journal of Geodynamics*, Vol. 28, No. 2-3, 131-145.
- Ma, C. and J. W. Ryan (1998): NASA Space Geodesy Program-GSFC Data Analysis-1998, VLBI Geodetic Results 1979-1998 (<http://lupus.gsfc.nasa.gov>).
- Shaffer, D. B. (1995): Geodetic Measurements with VLBI Very Long Baseline Interferometry and the VLBA, *ASP Conference Series*, Vol. 82, 1995, J. A. Zensus, P. J. Diamond and P. J. Napier (eds.).

